A&A 385, 600–618 (2002)
DOI: 10.1051/0004-6361:20020075

Astronomy & Astrophysics

The enigmatic WR46: A binary or a pulsator in disguise⋆

II. The spectroscopy

P. M. Veen[1], A. M. van Genderen[1], P. A. Crowther[2], and K. A. van der Hucht[3]

[1] Leiden Observatory, Postbus 9513, 2300 RA Leiden, The Netherlands
[2] Department of Physics and Astronomy, University College London, Gowerstreet, London WC1E 6BT, UK
[3] Space Research Organization Netherlands, Sorbonnelaan 2, 3584 CA Utrecht, The Netherlands

Received 1 September 2000 / Accepted 5 November 2001

Abstract. We present spectroscopic monitoring of the Wolf-Rayet (WR) star WR 46 between 1989 and 1998, which has been obtained simultaneously with multicolour photometry (Veen et al. 2002a, Paper I). The spectroscopic monitoring data show that the radiative fluxes of the optical emission lines (O VI 3811/34, O VI 5290, N V 4944, N V 4604/20, He II 4686, He II 4859, He II 5411, He II 6560) vary in concert with the photometric single-wave (sw) frequency $f_{\rm sw}$ (Paper I), and also the difference of that period between 1989 and 1991. The line-flux variability does not provide obvious support for a short second period (Paper I). The radial-velocity variations show a remarkable behaviour: usually, they display a coherent single-wave on the time scale of the double-wave period, while during some nights the radial velocity appears surprisingly to stay constant (see also Marchenko et al. 2000). These so-called stand-stills may be related to the observed time-delay effects. A time-delay effect manifests itself in several phenomena. Firstly, the line flux shows small, but persistent, time-delays for lines originating from lower optical depths, the outer-wind lines (N V 4604/20 and He II). Secondly, the radial-velocity variations display much larger time-delays than the line fluxes and their behaviour appears less consistent. *Assuming* that the double-wave period controls the radial velocity, the stand-still is observed to start when the radial motion is in anti-phase with the presumed orbital motion. Thirdly, the outer-wind lines are observed to enter a stand-still much later than the inner-wind lines. Fourthly, the radial-velocity variations of the peaks of the emission lines precede the radial-velocity variations of the wings of those lines. In addition to line-flux- and radial-velocity variability, the He II 4686 emission line shows pronounced line-profile changes on a time scale of hours. Our monitoring is not sufficient to study this in detail. Furthermore, we discern a flaring behaviour, i.e., an emission bump appeared on the blue wing of two He II-lines (around -1700 km s^{-1}) lasting less than 5 min. Finally, the line fluxes follow the observed brightenings, also on a time scale of years. We conclude that the short-term cyclic variability confirms the WR nature as established from the WR standard model analysis by Crowther et al. (1995; hereafter referred to as CSH). The various time-delay effects are consistent with the formation of the spectrum in a stratified stellar wind. The outer layers trail the inner ones. The variability is inconsistent with the formation of the spectrum in a stellar disc as proposed by Niemela et al. (1995) and Steiner & Diaz (1998). The long-term cyclic variability of the brightness and line fluxes is related to an increase of the mass-loss-rate, and, possibly, to the period changes. The interpretation of the nature of the variability is deferred to Veen et al. (2002b, Paper III).

Key words. stars: Wolf-Rayet – stars: individual: WR 46 – stars: binaries: close – stars: variables: general – stars: oscillations

1. Introduction

This is the second paper in a series of three, presenting the enigmatic variability of the Wolf-Rayet (WR) object WR 46 (HD 104994). In Veen et al. (2002a, hereafter Paper I) photometric monitoring of the object is presented and investigated. A double-wave character is revealed, although it is not very significant. Another remarkable conclusion reached in Paper I is that the period changed from $P_{\rm dw}^{89} = 0.2825$ d in 1989 to $P_{\rm dw}^{91} = 0.2727$ d in early 1991, while the object brightened gradually in the meantime by $0\overset{\rm m}{.}12$. Such a period-change is rather unsettling to the interpretation as a binary. Alternatively, the system could be a multi-mode pulsator showing different modes in different epochs. Also the occurence of a photometric second frequency $f_{\rm x}$ (Paper I) can be explained in a natural way by such a model. Yet, the large radial-velocity amplitude and its typical time scale on the order of the

Send offprint requests to: A. M. van Genderen,
e-mail: genderen@strw.leidenuniv.nl

⋆ Based on observations collected at the European Southern Observatory (ESO), La Silla, Chile.

photometric double-wave is, in turn, problematic for this interpretation. Full consideration of both models is deferred to Veen et al. (2002b; hereafter Paper III).

In the present paper we investigate the spectroscopic variability of WR 46 and show it to be consistent with a true Population I WR nature. The following section presents the data of five years of spectroscopic monitoring in the last decade, obtained simultaneously with our photometry (Paper I). Section 3 presents the line flux and radial-velocity measurements. In Sect. 4 we present the temporal behaviour of the spectral data, i.e., folded radial-velocity and *EW* curves, time-delays, two (possibly) non-periodic phenomena, and the long-term behaviour. Section 5 discusses the WR nature of the object. Section 6 summarizes all available spectroscopic observations and their inferences. For the observational history of the object we refer to Paper I, and for the issue of how the variability of WR 46 relates to that of other WR stars we refer to Paper III. Our interpretation of the observed spectroscopic and photometric variability is presented in Paper III.

2. Observations and reduction

Our spectroscopic data were obtained with the ESO 1.5-m telescope, equipped with a Boller & Chivens spectrograph. The spectra were recorded on a CCD and reduced with MIDAS (NOV95). The data were bias- and flatfield-corrected. Cosmic-ray hits were removed automatically in the background, and by visual inspection in the spectrum. Subsequently, the spectra were optimally extracted (Horne 1986).

During the 1989, 1990 and 1991 runs, the exposure time was 3 min and the spectra were obtained in sets of 10, followed by a HeAr wavelength-calibration frame. Table 1 lists the specific details of each run. To perform a radial-velocity study, we rectified the spectra. We used the telluric line at 5578 Å and the interstellar lines at 5990, 5995 Å to correct for possible systematic offsets in wavelength calibration. Offsets occured up to 100 km s^{-1}, a fraction (1/6th) of the resolution (2 pixels). Note that other (weaker) telluric lines were removed during the background subtraction.

The 1995 and 1998 spectra were taken with a holographic grating, resulting in a dispersion of 0.5 or 1.0 Å per pixel. The exposure time was 30 min. After each spectrum an HeAr calibration frame was obtained. In these spectra the so-called "blue fringing" occured, which is a familiar problem of the optics of the ESO 1.5-m telescope at high resolution, which cannot be corrected for. Due to this effect the He II λ5411 line in the 1995 data became distorted and in 1998 the continuum between N V λ4944 and O VI λ5290 was affected.

3. Results

A rectified echelle spectrum of WR 46 by Hamann et al. (1995b) is shown in Paper I (their Fig. 14). We note that according to Smith et al. (1996) the N IV 3480 emission line is only faintly present, while a spectrum by Massey & Conti (1983) does show this line on the edge of their spectrum with a intensity of 0.2 in continuum units. Crowther et al. (1995, hereafter CSH) showed the spectrum to be similar to other weak-lined early-type WN stars, e.g. WR 128 (WN4(h)) and WR 152 (WN3(h)) (spectral types of Smith et al. 1996). The differences are that WR 46 shows no sign of any hydrogen, the N V (resp. He II) lines are stronger (resp. weaker) and the wings are somewhat broader as a result of a faster wind. CSH modeled the observed triangular line profiles assuming a spherical, low-density WR stellar wind. We note that the spectrum of WR 3 (HD 9974, WN3) is very similar to that of WR 46 (Marchenko priv. comm.), except for the O VI 3811/34 emission lines, which are absent in WR 3, but very prominent in WR 46. The discussion of this feature is deferred to Sect. 5.2.

Table 1. Observers of spectroscopic data sets obtained at the 1.5-m ESO telescope with a Boller & Chivens spectrograph attached. The third column lists the spectral dispersion d in (Å/pix).

Observer	date	d	λ(Å)	S/N
H. E. Schwarz	13–15/3 1989	5.4	4100–7150	125–200
H. E. Schwarz	28/2–2/3 1990	5.4	4100–7180	140–215
M. Verheijen	15–17/2 1991	3.7	3700–7300	130–250
P. M. Veen	2, 4/4 1995	0.5	3785–4785	50–60
	3, 5/4 1995	1.0	4715–6735	70–110
P. M. Veen	10–11/2 1998	0.5	4750–5700	100
	12/2 1998	0.5	4900–5840	100

To illustrate the variable behaviour of the spectral lines we present a gallery of grey-scale figures of various lines observed in different years. These figures show either the same line on different nights (Fig. 1), different lines of different elements during a single night (Fig. 2), the same element and ionization (Fig. 3) during subsequent nights, or both (Fig. 4). We discuss the characteristic behaviour of WR 46 in the N V 4944 emission line. This line shows both an obvious radial-velocity curve (e.g., the second night in 1998 (Fig. 4), or the fourth night in 1995 (top panel of Fig. 3)), and, a stand-still with, or without, a change of flux (e.g., second night in 1995, Fig. 4).

3.1. Continuum-corrected equivalent width ($EW_{\rm cc}$)

We introduce a new variable, the so-called continuum-corrected equivalent width $EW_{\rm cc}$, which measures the line flux relative to the continuum of a specific spectrum, which was chosen to have truly simultaneous photometry available (V_0 with $\Delta t < 3$ min) near the mean brightness. First, the different lines with adjacent continuum are extracted and rectified using a first- or second-order polynomial. Then, we measure the standard equivalent width relative to the continuum of the spectrum itself. Since the emission lines contribute only <10% to the broad-band

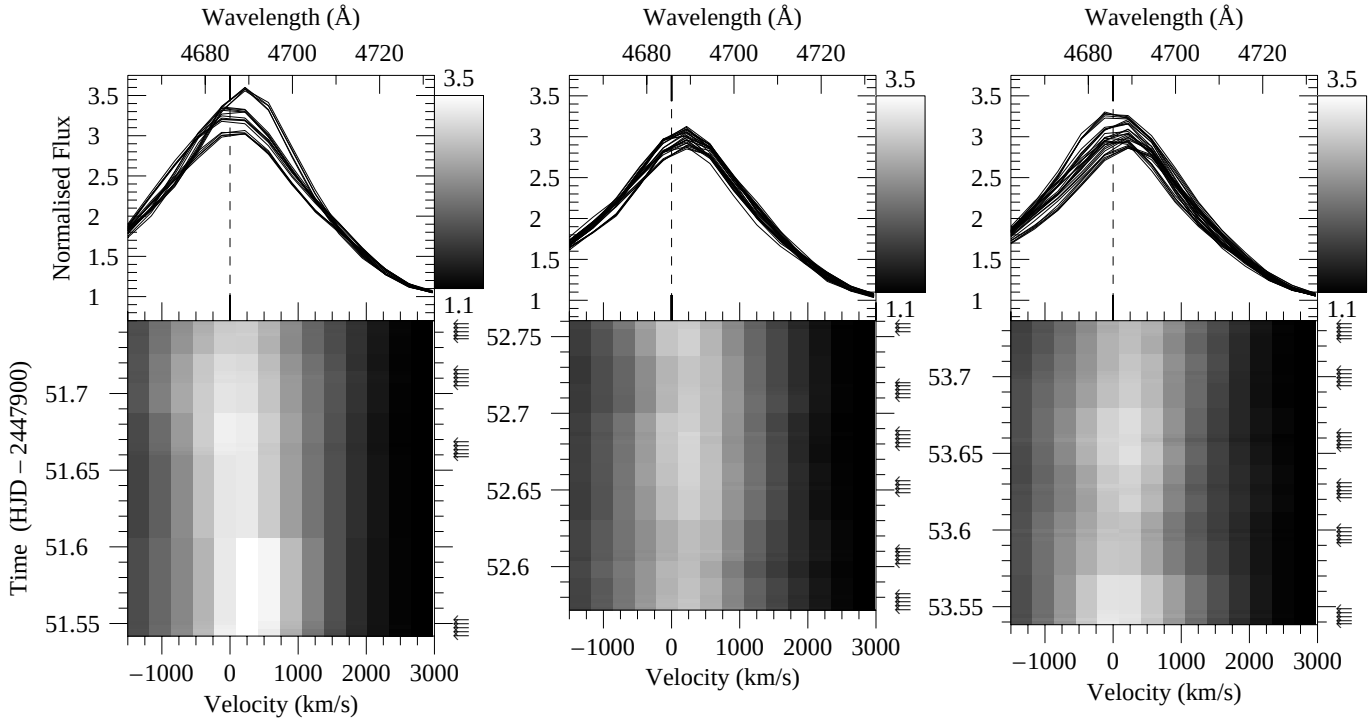

Fig. 1. Three nights of observing the He II 4686 emission line at low resolution (28 Feb., 1, 2 Mar. 1990) illustrate the variability from night-to-night.

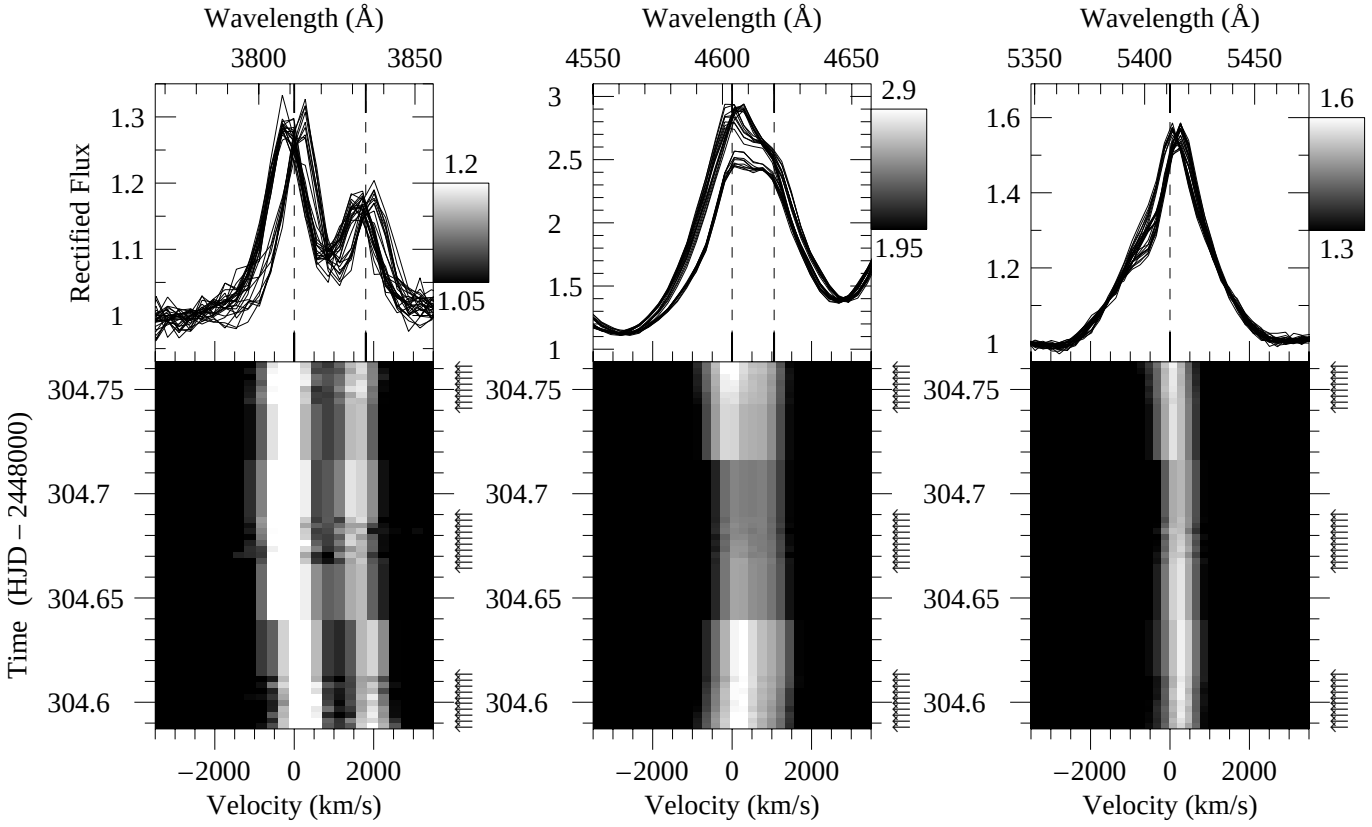

Fig. 2. Simultaneous behaviour of (from left to right) the O VI 3811/34, N V 4604/20 and He II 5411 emission lines during the night of 16–17 February 1991.

Table 2. The ratio of the maximum over the minimum flux within different pass-bands during the days of simultaneous observations (corrected for the varying emission-line contribution) and the ratios of the maximum over minimum EW_{cc} (i.e., corrected for continuum) of the emission lines.

emission	1989	1990	1991	1995[a]	1998
W	1.03		1.047		
U			1.047		
$U_{B/J}$					
L	(1.0)		1.048		
B	1.04		1.060		
V	1.05		1.069		
O VI 5290				1.22	1.37
O VI 3811/34			1.54	1.39	
N V 4944	1.36	1.43	1.47	1.51	1.29
N V 4604/20	1.66	1.71	1.38	1.37	
He II 4859	1.78	1.77	1.38	2.25	1.17[a]
He II 5412	1.33	1.53	1.26	1.20	1.27
He II 6560	1.26	1.45	1.17	1.23	
He II 4686	1.25	1.33	1.16	1.21	

[a] Coverage during two nights only.

photometry, the EW of all the lines can be transformed to EW_{cc}, according to:

$$EW_{cc}(t) = 10^{V(t)-V_0} * EW(t), \quad (1)$$

where V is in $\log I$. The photometry is simply linearly interpolated to the times of observation of the spectra $V(t)$. The V-band is used, as it measures the continuum around He II 5411 accurately (see Paper I, Fig. 14) and the color changes are only very small and do not affect the following analysis. In effect, EW_{cc} reflects purely the changes in the line flux. By this approach the problem of absolute calibration is avoided, while the variability is unraveled from the continuum variations. Moreover, since the specific spectrum is chosen to be near the mean value of an observing run, the values can still be compared to other observing runs as "standard" EW.

Figures 5–9 present simultaneous measurements of the light curve (top row) and the EW_{cc} of several lines (middle part) and the radial velocity (bottom part) separated by thick lines. It is obvious that the line fluxes vary on the same time scale as the light curves and that their behaviour is comparable, i.e., their maxima and minima coincide roughly. Such behaviour is already apparent from the EW values, but evidently enhanced when corrected for the continuum contribution. The temporal behaviour is analysed in Sect. 4.

We determine the ratios of the maximum over the minimum flux-level of the continuum and the main emission lines for each observing run and the results are listed in Table 2. Because of the low number of cycles (2–3) observed per season, the determinations can only serve as a relative measure, since all lines (and continuum) are observed simultaneously. The table is ordered from the inner to the outer layers of the atmosphere and shows as trend that the amplitude increases when going outwards, out to

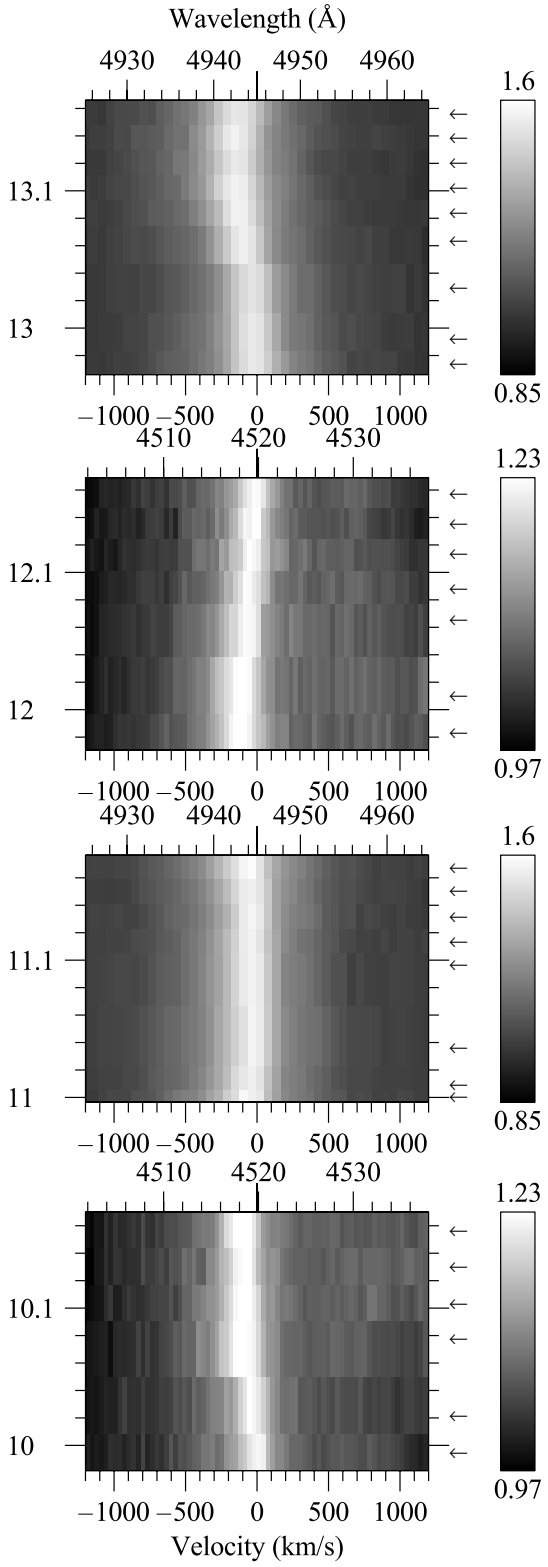

Fig. 3. The variability of the N V lines in four nights in 1995 (time HJD-2 449 800 running upwards). The 1st (bottom) and 3rd panel show the N V 4520 emission line, and the 2nd and 4th (top) panel show the N V 4944 emission line. They illustrate the radial-velocity variability and the abrupt changes from night to night. Although these lines originate from different principal quantum levels (n = 9–7 and 7–6, respectively), they trace nearly the same atmospheric region according to Wolf-Rayet Standard model analyses by one of us (PAC).

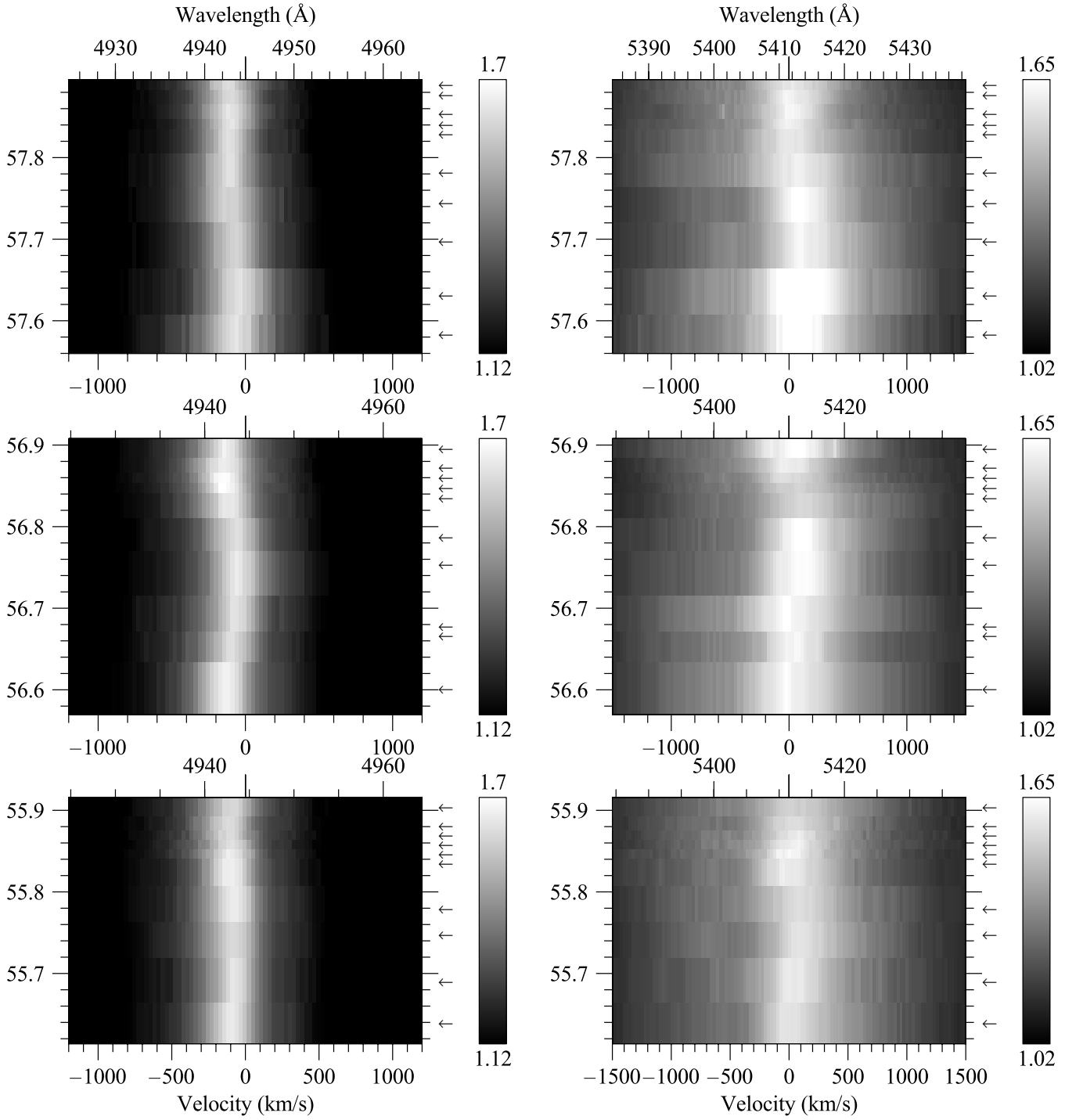

Fig. 4. Three nights (time measured upwards) of observing N v 4944 (left) and He ii 5411 lines (right) in 1998 illustrate the variability from night-to-night and the differences in radial velocity behaviour between the N v and He ii lines.

the formation region of either the spectral line He ii 4859, or, in 1991, O vi 3811/34. Further out, the ratio of the line fluxes decreases, presumably, as the effect of the variable source wears out due to a larger distance. In Paper III, this change of amplitude dependent on the height in the atmosphere is interpreted as a change of the distortion of the (line- and continuum-) emission-forming layers. The measurements of these ratios are translated into a graphical representation in Fig. 1 of Paper III.

3.2. Bi-sectorial radial velocity, K-amplitudes

We measure the bisector (i.e., the line center for each line) at three different intensities above the continuum, namely at 20, 50 and 85% of the maximum line intensity. A similar method was applied to WR 6 by Robert et al. (1992). We check the stability of the wavelength calibration by measuring also the interstellar and atmospheric lines. A systematic offset was notable only a few times, which we

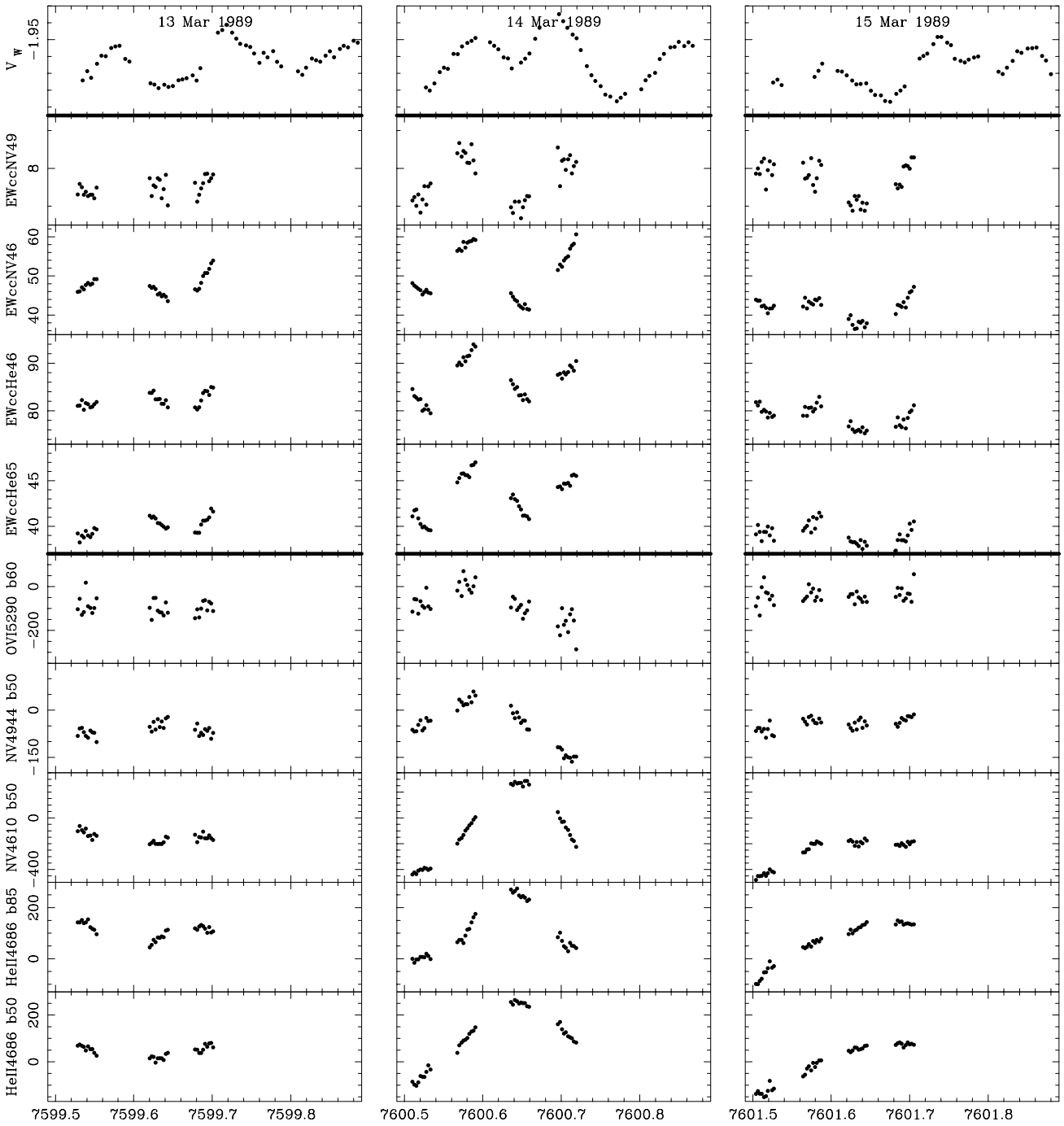

Fig. 5. *Top row:* Walraven V-photometry versus HJD$-2\,440\,000$ obtained simultaneously with spectroscopy (lower panels); *rows 2 to 5:* equivalent width corrected for continuum changes (cc; see Sect. 3.1) in Angström; *rows 6 to 10:* radial velocity in $\mathrm{km\,s^{-1}}$ measured as bisector at the specified height above continuum as percentage of the maximum flux (b50, b85, b60) during three nights in 1989 as indicated. The different emission lines (top down) are shown with increasing distance of its formation region from the star. Note that for some events the variability shows, among other changes, a clear time-delay increasing when going outwards.

subsequently corrected. The square root of the variance of these measurements (after correction) may be considered as error estimates for each data set: 30–50 $\mathrm{km\,s^{-1}}$ in 1989–91 and 3–5 $\mathrm{km\,s^{-1}}$ in 1995 and 1998.

The determinations are presented in the lower half parts of the Figs. 5–9. As already mentioned from the grey-scale graphs, the radial velocity behaves peculiarly. During one night the radial velocity shows a large-amplitude curve (e.g., 14 March 1989, 17 February 1991), while during another night it shows a stand-still (13 March 1989, 10 February 1998). Although the radial-velocity curve is not stable from night to night, showing a variable amplitude, it is clearly controlled by a time scale similar to the double-wave period of 0.2727/0.2825 d. We observe that in

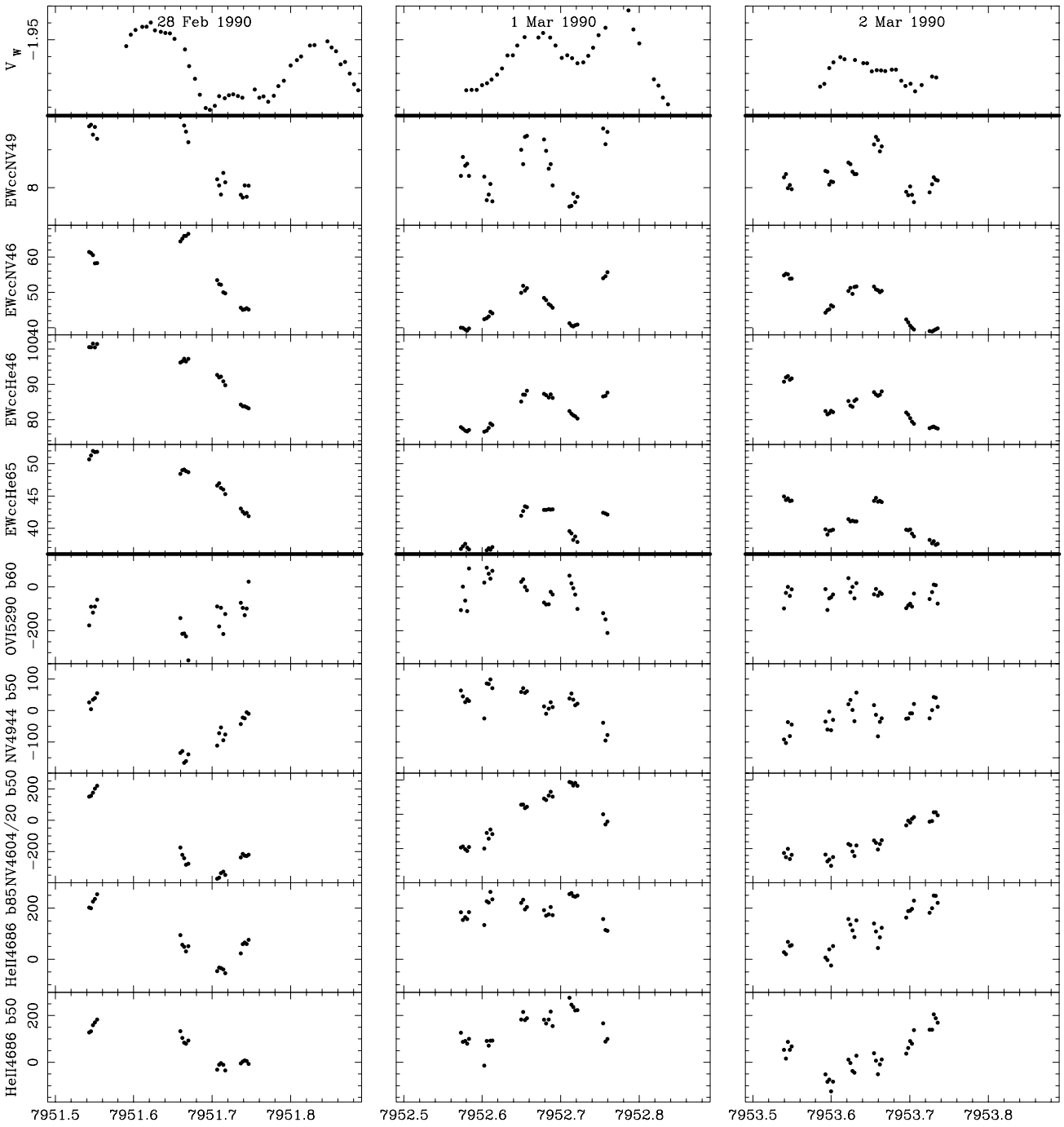

Fig. 6. As in Fig. 5, but for the 1990 data.

the case of a large-amplitude radial-velocity variation, the object is usually brightest, showing the largest line fluxes when the lines (formed in the inner wind region) are *either* at maximum velocity *or* minimum velocity. This relative timing can also be recognized in the 1999 data described by MAB. However, a counter-example may be the night of 1 March 1990 (Fig. 6), where N v 4604/20 shows the line flux to be minimal during extreme radial velocity.

We conclude that the radial-velocity amplitude for most emission lines is in the range $K = 50$–$100\,\mathrm{km\,s^{-1}}$. We assume that the lines formed closer to the WR star give a better indication than the N v 4604/20 line complex, which results in an outstandingly high amplitude of 250–300 $\mathrm{km\,s^{-1}}$. Such a large amplitude for this line-complex has also been observed by Niemela et al. (1995). Discussion of this phenomenon is deferred to Sect. 5.2.

4. Temporal behaviour

4.1. Time-delays in the spectral features

The upper panels of the Figs. 5–9 present the various emission-line flux curves at increasing distance from the stellar core (downwards). Inspection of these measurements from individual nights suggests that the time series

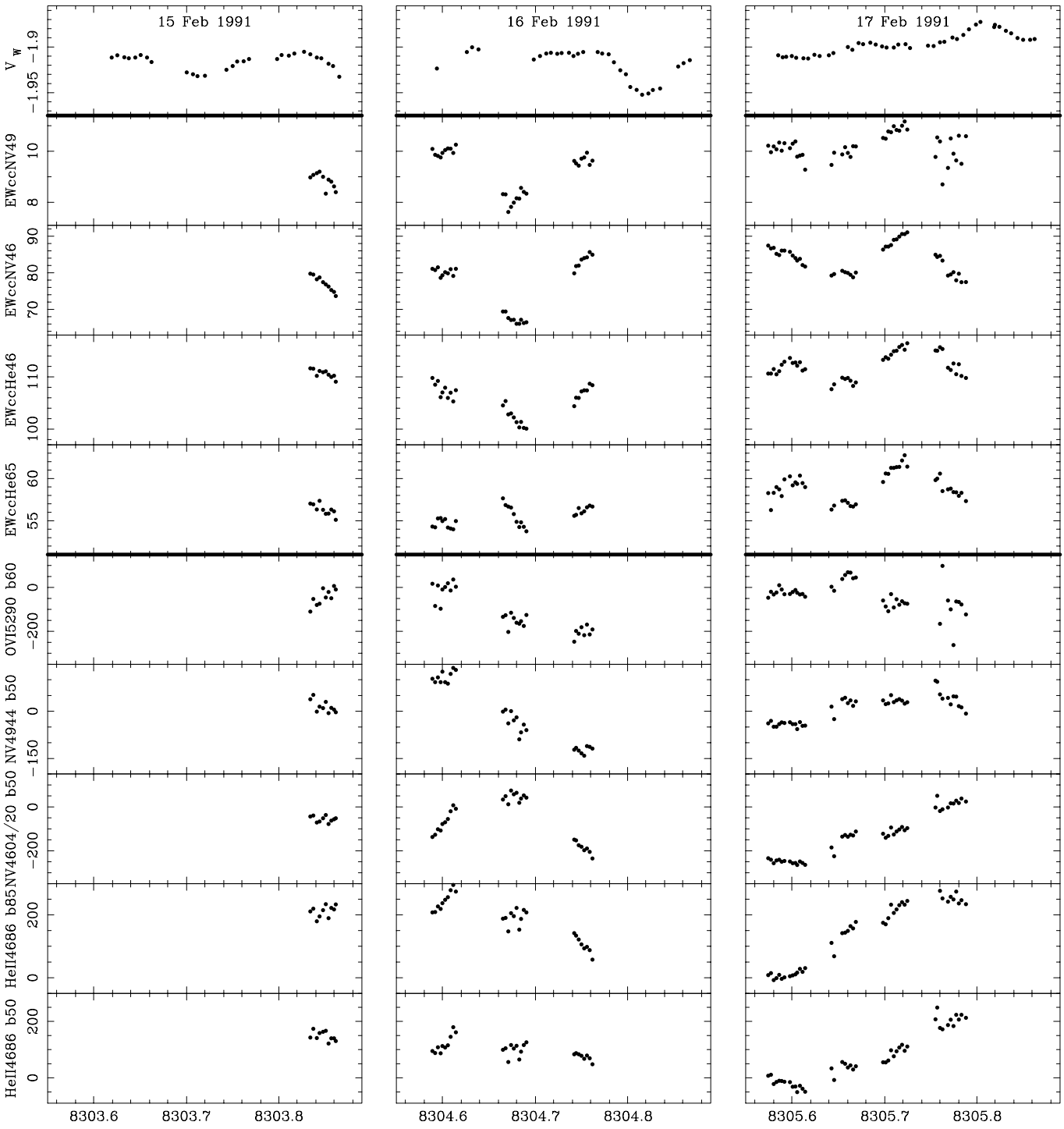

Fig. 7. As in Fig. 5, but for the 1991 data.

of the fluxes of the lines formed in the outer wind show, consistently, small time-delays with respect to the lines formed in the inner wind. For example, during 14 March 1989 the N V4944 line flux around t (HJD) = 2447600.65 has passed the minimum, N V4604/20 is about to enter the minimum, and the He II lines are still decreasing rapidly. More such cases can be observed. To determine the average value of a time-delay between two different emission lines, we perform a cross-correlation of the time series.

We apply the cross-correlation technique of Edelson & Krolik (1988), as implemented into the MIDAS Time Series Analysis context, to the emission-line flux curves in 1989, 1990, and 1991. When the correlation peak is well-defined (e.g., Fig. 12), the top of the correlation function is determined by fitting a second order polynomial. The resulting time-delays are listed in Table 3. The mean delay between two time series appears to vary from 0.007 d (10 min) to more than 0.02 d (30 min). Moreover, the delays in 1990 and 1991 are longer than in 1989, possibly related to

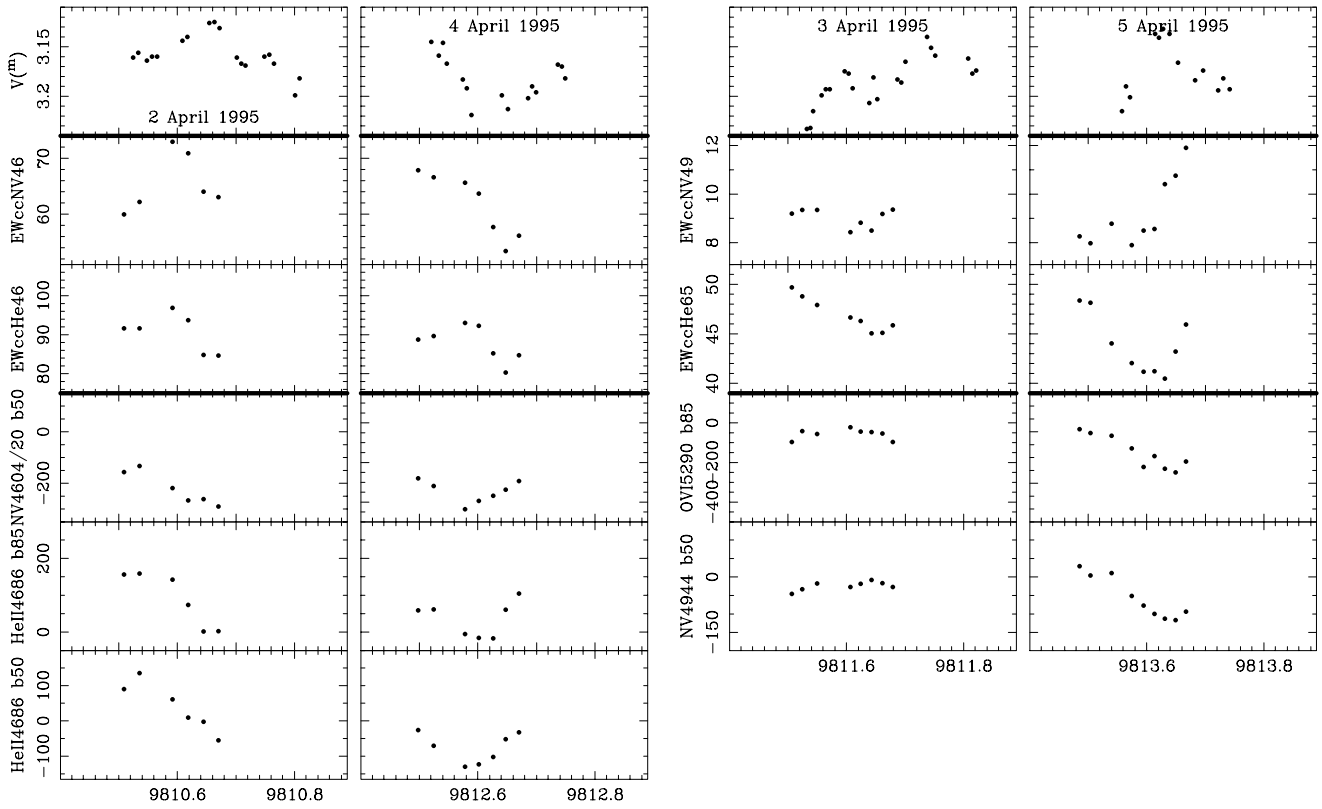

Fig. 8. As in Fig. 5, but for the 1995 data. Note that the nights are not presented as a time sequence.

the accompanying brightening. The largest time-delay is reached by the He II lines with respect to N V 4944, confirming the WR standard model that the latter originates deeper in the stellar wind. The cross-correlation of the helium lines amongst each other did not result in a peak significantly different from zero.

The time-delays of the radial velocity behave in the same sense as the line fluxes (outer wind lines delayed with respect to inner wind lines), but they are often much larger. An illustrative example is given by the observations in the night of 14 March 1989 (Fig. 5), where the maximum radial-velocity changes from around time $t(\mathrm{HJD}) = 2447600.58$ to $t(\mathrm{HJD}) = 2447600.64$, thus a delay of $0\overset{\mathrm{d}}{.}06$. The same amount of delay is found in the night of 28 February 1990 (Fig. 6). Thus, the radial-velocity time-delays can be three times larger than the line-flux time-delays, and, thereby, become a significant part of the typical time scale of variation. We did not perform the cross-correlation for the radial-velocity data, since the behaviour of the radial velocity is not as persistent as that of the line flux.

Yet another kind of time-delay is apparent on the night of 15 March 1989 (Fig. 5). On that night, evidently, the inner-wind lines are standing still, and it appears that with a delay of up to 0.15 d the outer-wind lines cease to move also. Apparently, the outer-wind lines trail the behaviour of the inner-wind lines also with respect to the entry of a stand-still.

In addition to the persistent line-flux time-delays, the variable radial-velocity time-delays and the delayed entry of a stand-still, we present also a line-profile time-delay. This concerns the bisector measurements of the same line but at different heights above the continuum. The top of the line precedes the lower parts: for instance, the 17 February 1991 He II 4686 bisector at 50% (Fig. 7) reaches its extreme values roughly 0.04 d later than the bisector at 85%. Figure 13 presents time-delay measurements of several emission lines from different seasons measured at different heights above the continuum, using the same cross-correlation technique as above. The observations clearly indicate that the lower parts of the emission line are trailing the peak of the line. This behaviour is not always noticeable in the available data, but, if it occurs, it is systematically in the same direction.

We conclude that all the stellar emission lines of WR 46 vary in concert, albeit with sizable time-delays. Also in the data by MAB (their Fig. 1, bottom panel) one can clearly notice a time-delay from O VI 3811/34 to N V 4944 out to the highest optical emission lines of WR 46. Both the time-delays from line to line, and within one line depending on the height above the continuum, are indicative of the stratification of the formation regions of the emission lines. Inferences are made in Sect. 5 and Paper III.

4.2. Relation with the photometric periods

The time-coverage of the spectral monitoring is not extended enough to perform an independent frequency analysis. To investigate the consistency of the line-flux variability with the photometry we folded the data with the

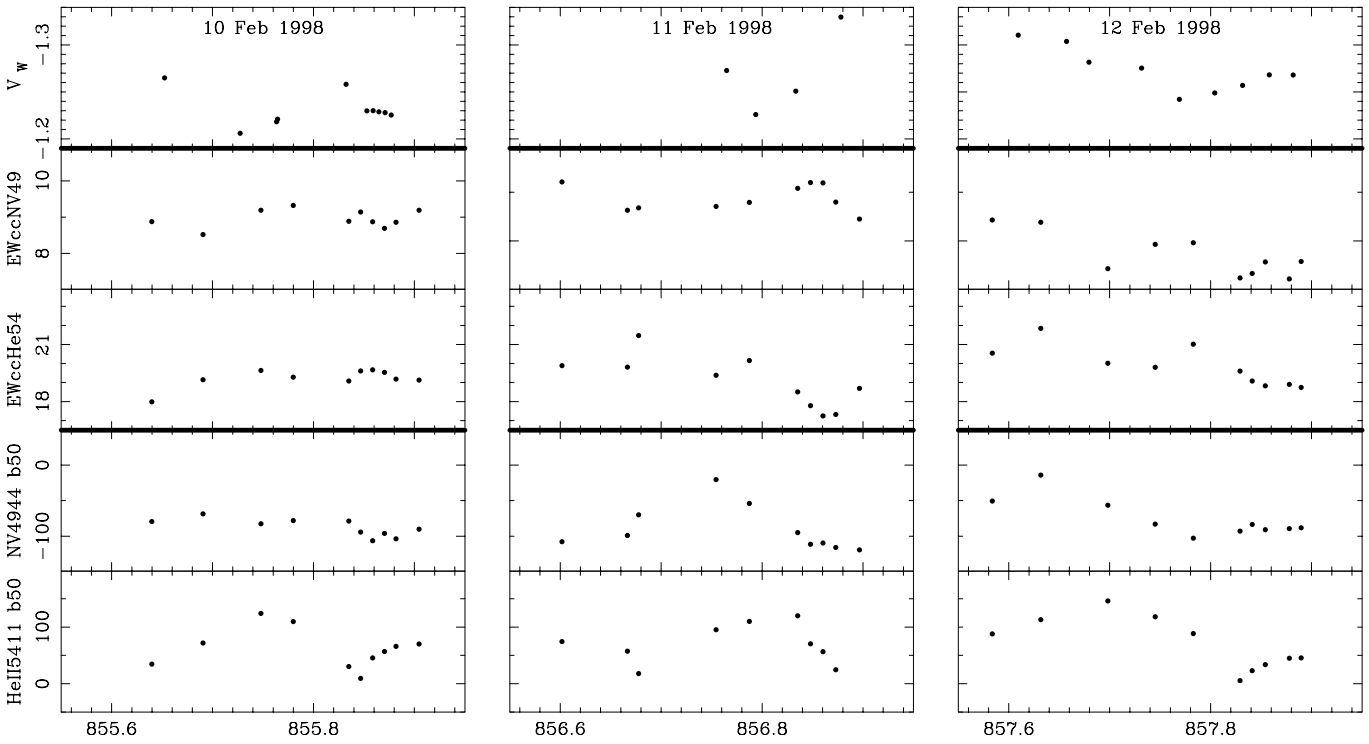

Fig. 9. As in Fig. 5, but for the 1998 data. Time is measured as HJD-2 450 000.

Table 3. Time-delays between various EW_{cc} curves. Column 1 lists the two emission lines for which the EW curves are cross-correlated (*). Columns 2–4 list the resulting time-delay, measured as the peak of the cross-correlation function. Positive numbers indicate a lag of the first mentioned spectral emission line with respect to the second line. The uncertainty in the last digits (bracketed) is the uncertainty of a parabolic fit to the top of the cross-correlation peak. (N v 4610 ≡ N v 4603/20).

lines	1989 (d)	1990 (d)	1991 (d)
He ii 4686*N v 4610	0.0071(08)	0.0115(23)	0.0131(34)
He ii 6560*N v 4610	0.0100(30)	0.0212(44)	0.0147(31)
He ii 4686*N v 4944	0.0112(75)	0.036(17)	0.025(11)
N v 4610*N v 4944	–	–	0.025(02)

Table 4. Fundamental parameters resulting from WR standard model spectral analysis. The results are based on the helium lines plus either the oxygen spectrum (CSH), as indicated in the last column, or the nitrogen spectrum (CSH and HK).

object	$T_\star$ kK	$R_\star$ $R_\odot$	$\log L$ $L_\odot$	$\log\dot{M}$ $M_\odot$/yr	v_∞ km s^{-1}	model
WR 46	91	2.4	5.5	−5.1	2450	CSH-O
WR 46	80	3.0	5.6	−5.3	2450	CSH-N
WR 46	89	2.2	5.4	−4.9	2300	HK-N
WR 3	89	2.5	5.6	−5.1	2500	HK-N

frequencies identified in the photometry (Paper I): the so-called single-, or double-wave periods $P^{89}_{\rm sw} = 0.1412$ d, $P^{91}_{\rm sw} = 0.1363$ d, $P^{89}_{\rm dw} = 0.2825$ d, and $P^{91}_{\rm dw} = 0.2727$ d which affect both the magnitude and the colours, and a secondary frequency, the so-called $f_{\rm x}$, with a period $P_{\rm x} = 0.2304$ d which affects only the magnitude. Figure 10 shows the folded line-flux curves of N v 4604/20. It does not provide any support for $f_{\rm x}$. Yet, the line fluxes in 1989, 1990 and 1991 appear well-behaved with the corresponding single- and double-wave frequencies (compare the neighbouring panels in Fig. 10). The 1995 line-flux data appear to show a single-wave, similar to the photometry in 1995. These data show only marginal preference for the 1991-period. As the 1998 data lack the N v 4604/20 line, the results of He ii 5411 are presented. The line flux does not behave well with any of the frequencies, similar to the photometry. Clearly, the variability of the photometry (dominated by the continuum) and that of the line fluxes is intimately related.

We conclude that the line flux provides independent evidence for the difference of the periods in 1989 and 1991. The object varies from year to year, and from cycle to cycle, but we have only three nights per season (i.e., three cycles or parts thereof). Thus, we are affected by low number statistics. Therefore, we cannot investigate whether the double-wave provides a better description of the line-flux curve than the single-wave. In addition, we cannot search for possible differences in the amplitude between the different seasons as found for the photometry. However, the mean values of the line fluxes follow the photometric behaviour (see Sect. 4.5).

Analogous to the line flux in Fig. 10, Fig. 11 presents the folded radial-velocity curves using the double-wave periods identified in our photometric study (Paper I), and partly supported by the line flux (the two left columns

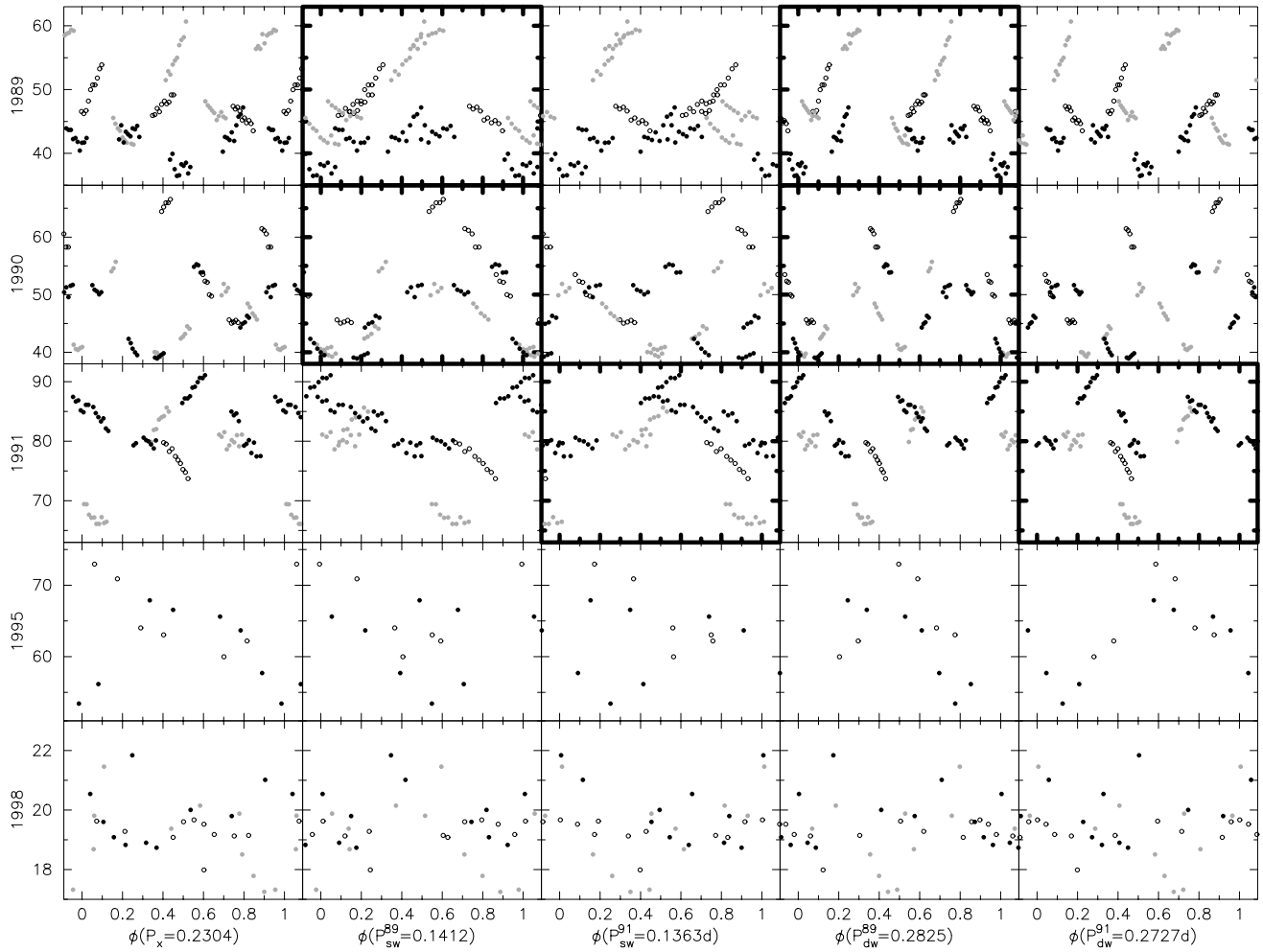

Fig. 10. Continuum corrected equivalent width ($EW_{\rm cc}$; see Sect. 3.1) in Angström of N V 4604/20 (and He II 5411 for 1998, bottom row) folded with the 1989 and 1991 periods ($P_{\rm x}$, $P_{\rm sw}$, $P_{\rm dw}$). The preferred curves are presented in the thick-lined boxes. Note that the vertical scale is adjusted to the observed range of $EW_{\rm cc}$ values. The different symbols indicate the sequence of the nights: open symbols the first; grey symbols the second; solid symbols the third night.

of the panels will be discussed below). While there is no satisfying match if $P_{\rm x}$ is used, the time scale of variability is, evidently, of the order of the double-wave period. However, the radial velocity is not strictly periodic with the photometric double-wave period.

We propose that this apparent a-periodicity of the radial velocity finds its origin in the large time-delays of the radial velocities. In fact, the observations of 15 March 1989 may hold a clue. During that night some lines show a stand-still, while others are on the verge of ceasing their radial motion. Precisely that night shows the largest apparent phase-delay, if $P^{89}_{\rm dw}$ is used. Thus, it is conceivable that if a time-delay becomes much larger than half a period, the radial motion comes to a stand-still.

We assume that the same mechanism does control the light-, the colour-, the line-flux-, and the radial-velocity variations with the double-wave periods. If this assumption is a correct, the photometric shallow minimum occurs during the change from maximum positive to minimum negative velocity. Furthermore, a frequency analysis of the radial velocity may be severely affected by time-delays and stand-stills, and it may identify unreliable, mostly longer, periods than the line-flux or photometric analysis would. The idea is that the stellar wind material cannot keep up with the stellar core and lags behind more and more. When the delay has built up to, say, half a period, the radial velocity averages out and the star enters a stand-still. In the course of time the atmosphere will pick up the radial motion again and for a few cycles display a radial velocity curve.

Since in our 1995 observations the radial velocity shows a coherent variability in three out of four nights (see Fig. 3), spanning the largest number of consecutive nights, we investigate its frequency spectrum. Similar as to the photometry, we apply the analysis of variance (AOV, Paper I) to a combination of N V lines from all four nights (λ4520 (9–7) and λ4944 (7–6)) and to a combination of He II lines (λ4686 (4–3) and λ5411 (7–4)). The resulting periodograms for the radial velocity are shown in Fig. 14. The highest peak appears at 2.7 cd^{-1} (P = 0.37 d), the same as in the photometry. This agreement between photometry and spectroscopy may indicate that the period

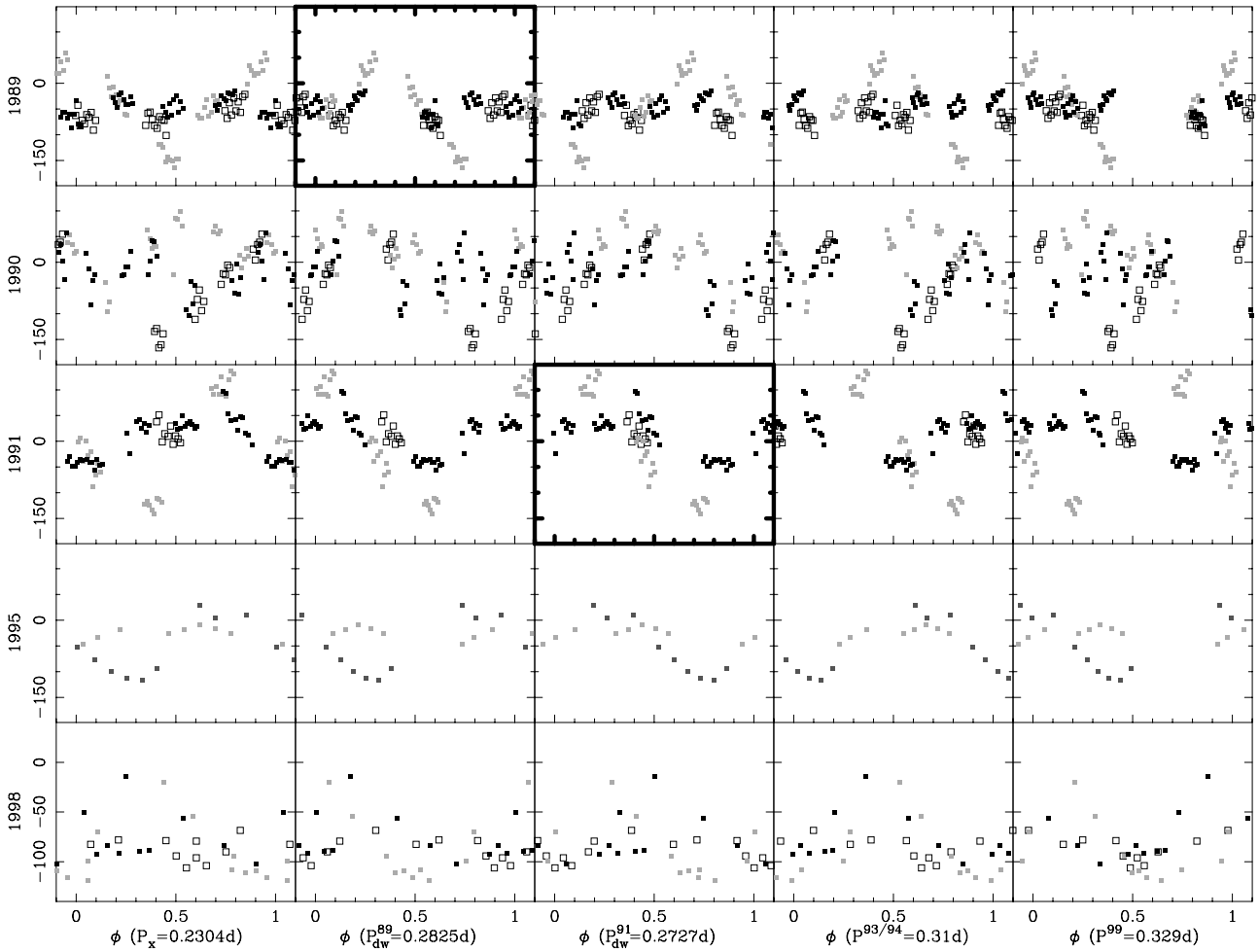

Fig. 11. Bisector at 50%-level of N V 4944 in $\mathrm{km\,s^{-1}}$ for all seasons folded with the various periods. From left to right we applied phasing with $P_{\rm x}$, $P^{89}_{\rm dw}$, $P^{91}_{\rm dw}$ (Paper I), $P^{93/94}$ (Niemela et al. 1995), and P^{99} (Marchenko et al. 2000; hereafter referred to as MAB). For the different fill styles see Fig. 10, and for 1995 dark-grey indicates the fourth night.

was indeed that large in 1995. However, both data sets are short, so we do not rule out the one-day alias at 3.7 $\mathrm{cd^{-1}}$, which coincides with the P_{91} as indicated in the insets in Fig. 14. Possibly, the variability is controlled by a period comparable to P_{91}, while the time-delay has larger significance for the longer-period aliases.

Other period determinations of WR 46 based on radial velocity measurements have been performed by Niemela et al. (1995), who found $P_{93/94} = 0.31$ d from observations in 1993 and 1994, and by MAB who found $P_{99} = 0.329$ d from 1999 data. Marchenko et al. (2000) remarked that the observations by Niemela et al. may be hampered by an apparent halt of the radial motion on one out of three consecutive nights. They conclude that both periods are compatible, while we conclude that both are not compatible with our measurements, as evidenced in Fig. 11.

These large variations of the period based on radial-velocity data (0.31 d in 1993/4, 0.27 d or 0.37 d in 1995, 0.329 d in 1999 and, probably, different from before in 1989 and 1991) support our suggestion that the radial velocity is too disturbed by time-delays and possible related standstills. In this interpretation the photometry, or, possibly, the line fluxes, provide a better tool to determine the period(s?) of the system than the radial velocity.

In summary: (i) the line flux follows the photometric behaviour, i.e., the photometric single/double-wave period is consistent with the line-flux variability, even to the extent that (ii) the substantial period change between 1989 and 1991 is supported; (iii) the 1995 period determined (semi-independently) from the spectra may be equal to P_{91}, also suggested by the photometry; (iv) the 1998 data confirm the time scale of variability, but the period cannot be derived with precision and may well have changed since 1995; (v) the large deviations between the periods determined by other investigators from radial-velocity measurements and our photometric determinations may either result from the large and varying time-delays, or they may indicate intrinsic large period changes.

4.3. Peculiar line-profile variability of He II 4686

Our high-resolution spectra show that the spectral variability may involve more than only line-flux and radial-velocity variability. Each panel in Fig. 15 shows

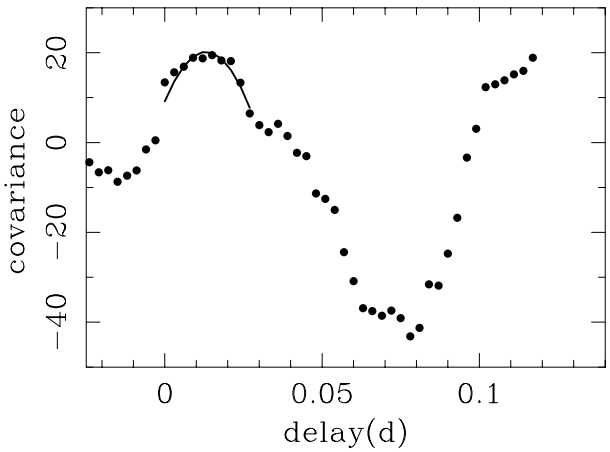

Fig. 12. Cross-correlation measurements of the time series of the equivalent width of He II 4686 and N V 4603-20. The maximum is fitted using a 2nd order polynomial and the hydrogen line is delayed by 0.013 d relative to the nitrogen emission line. Note that the covariance shows another maximum, a single-wave period later, as is to be expected.

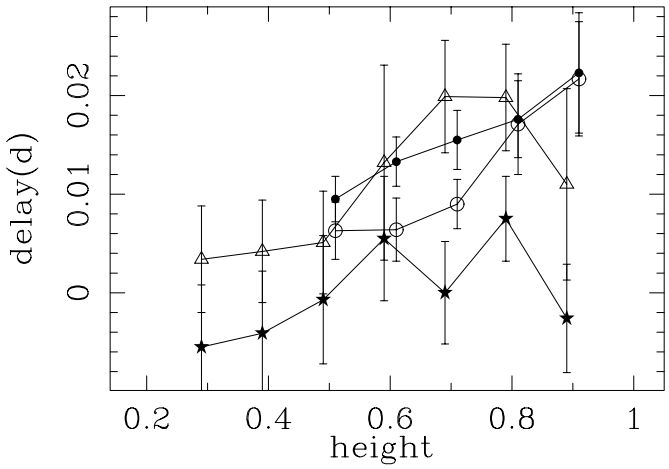

Fig. 13. Time-delay between radial-velocity curves derived at different intensities above the continuum versus height as a percentage of the peak. Several lines showing a significant lead by the peak are indicated (He II 4686: dots and N V 4604/20: circles on 17 February 1991 and N V 4944 on 4 April 1995: triangles), while a time series which did not show this behaviour is also indicated (N V 4944 on 11 February 1998: stars).

consecutive spectra on 4 April 1995. There is clear evidence for complicated line-profile variability of He II 4686 on a time scale of hours. The inner-wind lines (see Fig. 3) show simultaneously a large shift from negative to positive velocity. The time coverage is not sufficient to investigate the phenomenon any more deeply. Note that the line shows radial-velocity and line-flux variability (not shown) during the other night when observing the blue spectrum (2 April 1995).

At the risk of over-interpreting the data, we note that the profile variability can be described as a large and wide emission bump moving from the red wing to the blue wing over the peak of the He II 4686 line. That is consistent with

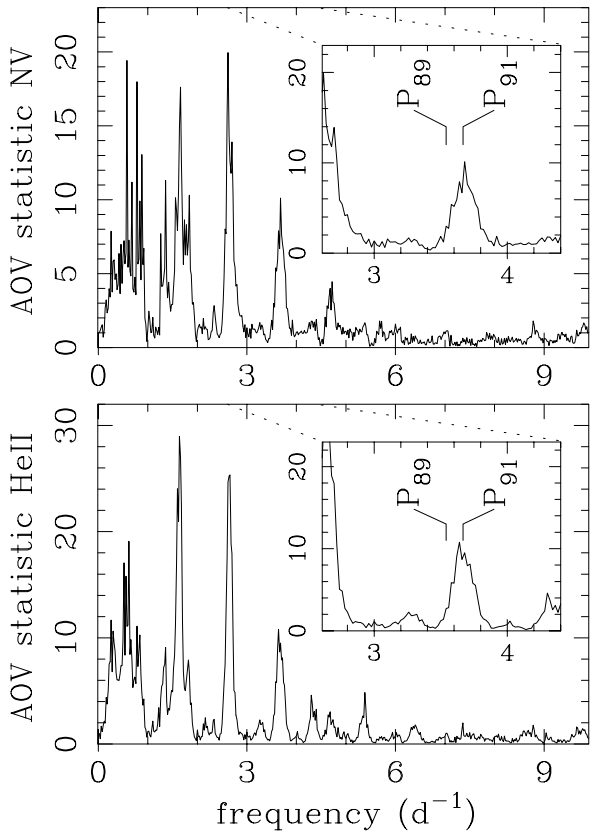

Fig. 14. AOV-periodograms of the radial-velocity measurements in 1995 of the N V 4944 and N V 4520 lines (*upper panel*) and of the He II 4686 and He II 5411 lines (*lower panel*). Evidently, one of the alias peaks is at the position of the 1991 period of 0.2727 d (=3.67 cd^{-1}).

the notion of an enhanced outflow from one side of the WR star. If this side is pointed away from the observer, the enhancement is red-shifted, and as the star rotates the enhancement is shifted over the peak to the blue wing.

4.4. A flare-like event in He II 5411 and 6560

In addition to the short-term brightness, line-flux, radial-velocity, and line-profile variability, we find evidence for a spectral variability on a time scale of minutes, or shorter. Figure 16 shows one of the sequences of low-resolution spectra observed on 15 March 1989 (exposure time of 180 s). Obviously, one of the spectra (7th out of 10) shows significantly enhanced localized emission (a "bump") on the blue wings of the He II 5411 (around -1600 km s^{-1}) and the He II 6560 (around -1800 km s^{-1}) lines, without notable changes to the rest of the profile. We note that the spectra observed directly before and after do not show any sign of such a "bump". As the time interval between the 180-s exposures is less than a minute, we derive an upper limit of the life-time of the local emission excess of 5 min. In the lower panel of Fig. 16 the difference between the mean of these latter spectra and the "bumpy" spectrum is presented. We inspected the raw data, but we do not observe any defects or cosmic ray hits. Moreover, we cannot

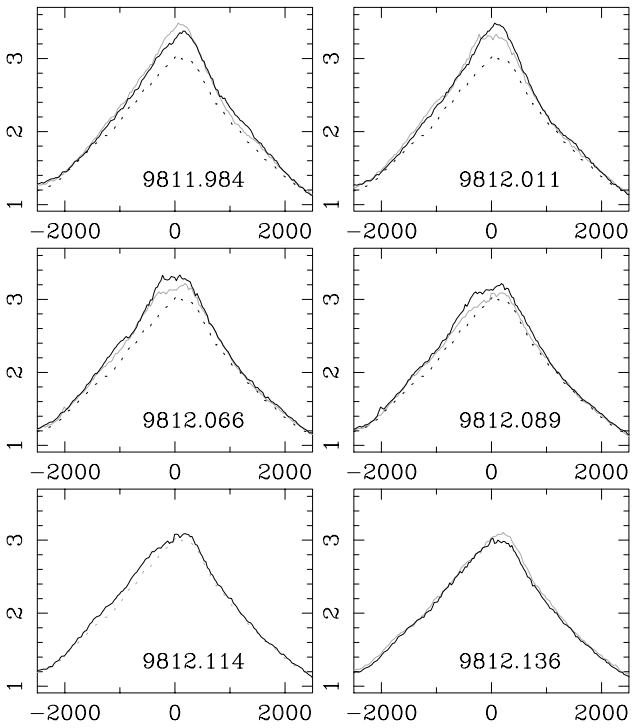

Fig. 15. The panels present (row-wise) consecutive observations of He II 4686 on 4 April 1995 (full lines) with the time of observation indicated as HJD-2 440 000. To allow easy comparison between subsequent spectra, each panel shows also the succeeding spectrum (grey). Moreover, to allow comparison over the whole night, the spectrum with minimal line flux (last panel) is repeated in each panel (dotted).

imagine any instrumental or telluric effect which would cause such an observation in two He II lines.

This flaring event occurred at $\phi = 0.1$ using the double-wave period, but we do not know whether this is significant. We searched the rapid monitoring data sets in 1989, 1990 and 1991, which amounts to about 18 hours of observing time, but found no similar feature. Obviously, such flare-like events are rare. We note that our high resolution data can not show such an event since the integration time is about ten times larger than the time scale of this variability.

4.5. Long-term spectroscopic variability

As discussed in Paper I, WR 46 varies also on a time scale of months to years. Figure 17 shows its accompanying long-term spectroscopic behaviour. In addition to the measurements of our spectra, we quote measurements from the literature (Smith et al. 1996, spectrum obtained in March 1988) and measurements of spectra kindly provided by others: the 1986 spectrum was obtained by Dr. W. Schmutz; the 1993 spectrum is part of the spectral atlas by Dr. W.-R. Hamann (Paper I, Fig. 14); the three 1994 spectra were provided by Dr. V. Niemela, see Niemela et al. (1995). Measurements of *EW* are notoriously subject to the determination of the continuum, which is problematic in WR spectra. The peak-to-continuum ratio is less affected for high peaks, thus, we also use these ratios.

The long-term behaviour of the *EW* of all emission lines from 1989 through 1991 varies clearly in concert with the photometry (Fig. 17). Therefore, we will use the terms "high state" indicating a high brightness with strong emission lines, and "low state" indicating the opposite. The 1993 spectrum indicates that the line fluxes declined like the photometric variation to a low state. The 1994 data are at a more intermediate level, and, therefore, more ambiguous. In 1995 the He II-lines are at a low level, in agreement with the hint of a low-state from the photometry, while the N V-lines appear to be strong. We note that the N V4604/20 line is sensitive to small variations in stellar temperature and mass-loss rate (Sect. 5.2). We assume that during the 1995 run the object was still in the low state. In 1998 the He II 5411 line indicates a high state, which fits the subsequent photometric decline a few months later. In 1999 the photometry indicates a rise, supported by the spectroscopy of MAB showing strong lines again.

As to the earlier years, both the photometric and the spectroscopic measurements in 1986 all agree to a low state, while the 1988 data are ambiguous. For the 1988 data Smith et al. (1996) list for the He II 5411 and the N V 4944 line the same *EW*, which is surprising. The N V 4944 line is narrower than He II 5411 as in all other spectra but it is stronger (L. Smith 2000, private communication), which is unique. Moreover, their *EW* of He II 4686 is very large, in contrast to their *EW* of He II 5411, which is in accordance with the low state evident from the photometry.

We also searched the literature for earlier observations of WR 46. Massey & Conti (1983) published a spectrum, probably observed in November 1981, on which we measured the peaks of the He II 4686- and N V 4604/20 lines at a value of 3.0 and 2.36 times the continuum, respectively, indicative of a low state. An earlier paper by Massey & Conti (1981) presents parts of yet another spectrum obtained before 1980, which shows a stronger N V 4604/20 line and a He II 5411 line peaking in the range of the 1991 data. The *EW* of He II 6560 dating from February 1982 (Vreux et al. 1983) is at an intermediate level compared to our measurements of He II 6560 obtained in 1989 through 1991 (not shown).

Additionally, the left-hand side margin of Fig. 17 shows measurements obtained by Smith (1955) in the early 1950s. Evidently, his values are the smallest ever. In addition, he noted that He II 5411 and He II 6560 are faint and broad. From other early observations (1949–1951), Henize (1976) classified the emission of the latter spectral line as weak to moderate relative to the continuum. Supposedly, this means that it was weaker than the present-day. Therefore, Fig. 17 may, tentatively, be interpreted to show also a rising trend on a time scale of decades to a century. Unfortunately, the photometric observations over the last century (Paper I: Table 1) cannot

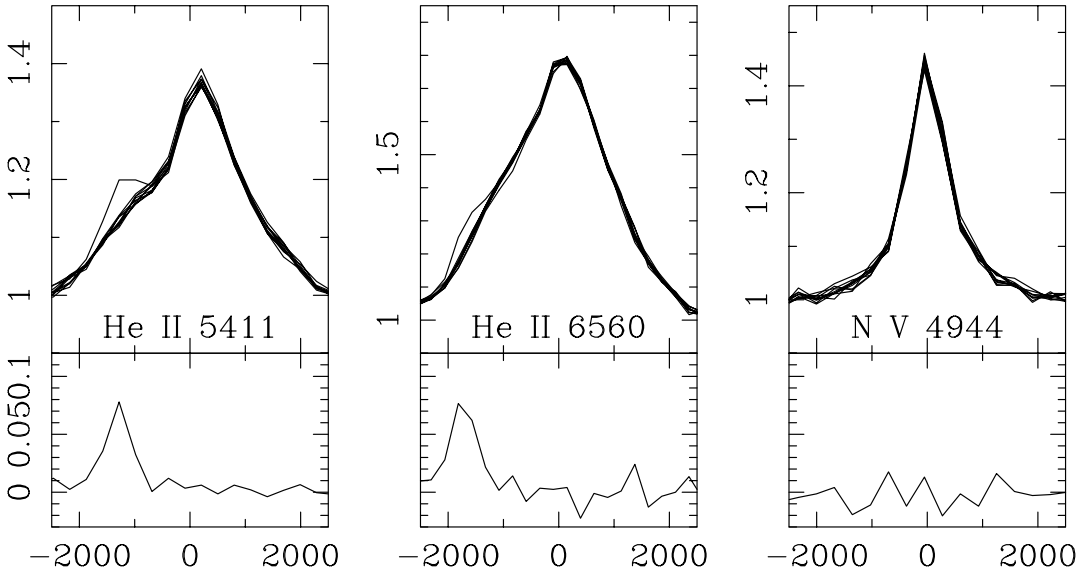

Fig. 16. Flare-like variability of two He II lines, but absent in N V 4944. Ten consecutive spectra with an exposure time of 180 s were obtained in low-resolution mode on 15 March 1989 (HJD 2446701.68 ... 1.72). The seventh spectrum in the row shows a significant sudden excess emission in the He II lines at 5411 Å (left) around -1600 km s^{-1} and at 6560 Å (middle) around -1800 km s^{-1}. Other emission lines in the spectrum do not show such minute-scale variability, as evidenced by N V 4944 (right). *Bottom panels:* difference between seventh spectrum and the mean of the preceding and following, which were observed with a spacing of only 45 s.

be used to assess this proposition due to the large uncertainties of the differences in the pass-bands and the contamination by line emission. Note that we established that WR 46 did not change its spectral type over the last century (Paper I: Sect. 2). It may be worthwhile to measure the line strengths in the oldest spectra from the photographic plates around 1900 available at the Harvard Observatory (Paper I).

As a last source for studying the long-term behaviour we used the *IUE* data base, which contains several single short- and long-wavelength range ultraviolet spectra obtained in high- and low-resolution mode between 1979 and 1991. Because of the faintness of WR 46, the exposure time in high-resolution mode equals the single-wave period. These spectra confirm the variability on time scales from days to years. However, the data are too scarce to allow a period determination. The last spectrum happens to be recorded during the high optical state on June 5th 1991 (Fig. 17). And, since it shows the strongest emission lines, the high state also applies to the ultraviolet part of the spectrum. Furthermore, Fig. 18 displays the O V 1371 emission line from several epochs. Evidently, the absorption trough is deepest during the high state, consistent with an increase of the mass-loss rate as argued in Sect. 5 on basis of the increased emission-line fluxes.

We conclude that the line flux varies also on the long-term time scale, in harmony with the photometry, evidencing variation of the mass-loss rate. Conversely, the small and large *EW* measurements indicate that the object underwent similar brightenings both before and after 1991. Furthermore, there is a hint in the N V 4604/20 *EW* data and from other early observations, that WR 46 is also varying on a time scale of several decades to a century.

5. The Population I Wolf-Rayet nature of the primary light source in WR 46

5.1. Wind versus disc(-wind) model

As mentioned in Paper I (Sect. 2), WR 46 has recently been grouped together with three other objects (Steiner & Diaz 1998). Their group of so-called V Sge stars shows highly ionized ions like N V and O VI. Apart from the short-term variability, the group has been defined by the intensity of the He II 4686 emission line being larger than Hβ. The objects are suggested to be related to the Super Soft X-ray Sources (SSS)[1] found in the Magellanic Clouds. The latter type of systems, all binaries, are considered to burn hydrogen steadily on the surface of a white dwarf, which is fuelled from an accretion disc at a near-Eddington rate (reviewed by Kahabka & van den Heuvel 1997). Association of WR 46 with SSS had been suggested earlier by Niemela et al. (1995). Those authors argued that the emission-line spectrum is formed in a luminous accretion disc in an evolved binary system.

However, there is strong observational evidence that a strong wind is the dominant feature of WR 46. First, two UV lines show a P-Cygni profile (Fig. 18, see also CSH). Second, our observations provide a wealth of time-delay effects, which are difficult to comprehend within the framework of a luminous disc, since the highest velocities would have to be produced at the inner edge of the disc. In contrast, the time-delays are easily reconciled as a result

[1] Note that an alternative view is expounded by Lockley et al. (1997) who explain the radio emission (*and* X-ray emission) of V Sge as originating in a colliding wind binary, in agreement with an optical study by these authors and by Gies et al. (1998).

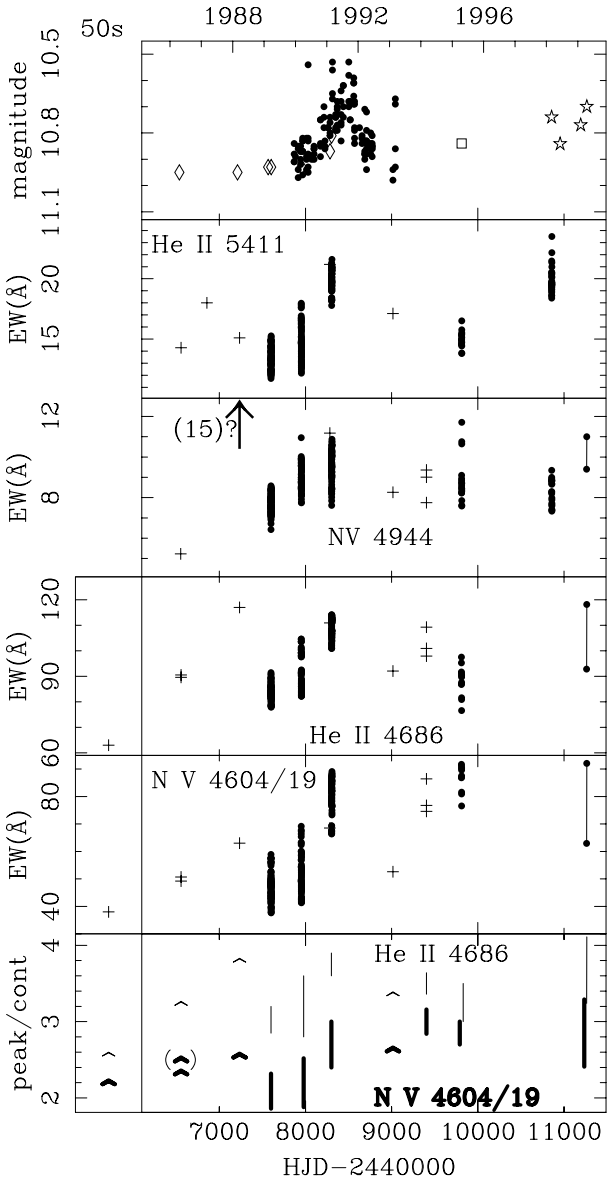

Fig. 17. Comparison between long-term photometric and spectroscopic variability. *Top panel:* long-term photometric light variation with symbols as in Fig. 13 of Paper I; *panels 2 to 5:* individual *EW* measurements (+) and sequences of *EW* measurements (dots); *bottom panel:* peak to continuum ratio's of emission lines as indicated individual measurements (ˆ) and full range as line-element.

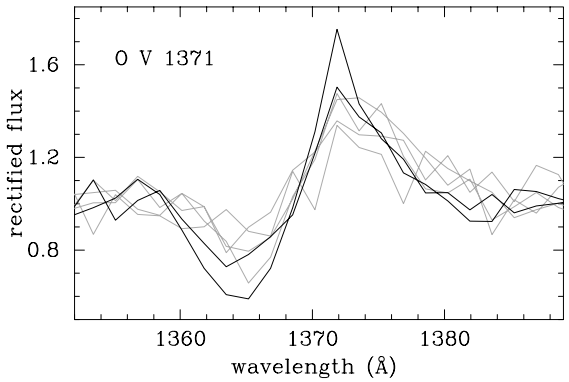

Fig. 18. All the short-wavelength *IUE* spectra of WR 46 display the O v 1371 line. Because of the large noise in the high-resolution spectra (black) due to its faintness, all spectra are resampled to the same low-resolution grid. The high-resolution spectrum showing the largest P-Cygni profile is observed incidentally at the time of the maximum brightness as recorded by *Hipparcos* (5 June 1991; see Fig. 17). The second high-resolution spectrum dates from October 1979. It is evident that the absorption trough of the 1991-spectrum is deeper, while the edge velocity is unaffected. The low-resolution specra (grey) confirm that the 1991 spectrum is in a "high state".

of a stratified atmosphere, where the pattern of variability travels outwards in an accelarating wind (Sect. 4.1). The apparent direct link between the continuum- and the line flux also indicates a common source of origin, as in the case of an optically thick wind.

In order for the disc-model to be consistent with these observations, it would be required to assume an optically thick wind from the disc. Such disc-winds are observed in the case of cataclysmic variables during nova-type outburst and thought to be driven by hydrogen surface burning (Kato & Hachisu 1994). Since WR 46 does not show hydrogen[2] (CSH; Hamann et al. 1995a; Massey & Conti 1981; note to the table by Smith et al. 1996 on marginal hydrogen presence can probably be disregarded, Smith private comunication), the donor star feeding the disc has to be a He-star, but without a WR wind. We consider this idea rather contrived, and conclude that the dominant light source in WR 46 is a Population I WR star blowing its own stellar wind. Also CSH and MAB reached this conclusion before. Possible binary companions of the WR star will be discussed in Paper III.

5.2. Variability of WR 46 within the WR Standard Model and the oxygen lines

CSH successfully applied their so-called "WR standard model" to WR 46. They were able to explain the whole UV to IR spectrum as a result of a rather low-density, spherically-symmetric, optically-thick WR stellar wind from a hot evolved star. We list the resulting fundamental parameters by CSH in Table 4 together with the results of a similar study by Hamann & Koesterke (1998; hereafter HK). Finally, the high luminosity of WR 46 is supported by the analysis by CSH of its interstellar lines. They derived a distance of 4 ± 1.5 kpc. For a more elaborate discussion on the distance to the system, the reader is referred to Veen & Wieringa (2000).

The colour behaviour of the system (Paper I: red when bright and blue when faint) is related to its high temperature. The spectral energy distribution peaks in the ultraviolet. Calculations using the "standard model" show that, if the temperature *increases*, at fixed bolometric

[2] Thus, the emission line at the position of Hβ, which is used to define the V Sge stars, is, in fact, a He II line.

luminosity, the visual continuum flux will decrease, as more flux will emerge in the EUV. Thus, the "peculiar" colour behaviour is completely understandable.

The variability of the N v 4604/20 line is much stronger than that of the neighbouring He ii 4686 line. This provides a nice illustration of its WR nature since the two fits by CSH (see their Fig. 6) show that N v 4604/20 is more susceptible for changes in temperature and mass-loss rates. We conclude that the short-term variability of the photometry and the line fluxes indicates a varying *local* density distribution in the wind.

So far, we ignored one peculiarity that emerged from the analysis by CSH. In their modelling the oxygen abundance appears three times larger than for the two other weak-lined WNE stars (WR 128 and WR 152) in their study. CSH argued that the oxygen content is not due to imperfections of the model, but truly anomolous, since the stellar parameters of WR 3 (Hamann et al. 1995a) are nearly identical to those of WR 46 and it does not show the O vi3811/34 line[3]. However, analyses of other stars by one of us (PAC) have shown that the O vi 3811/34-doublet is more susceptible to low wind-density. Thus, a more proper abundance indicator is the ratio of O vi 5290 to He ii 5411. Figure 19 shows these emission lines of WR 3 (grey) scaled to those of WR 46 with a factor of 2.5. Clearly, the ratio of these emission lines is very similar, thus the peculiar oxygen abundance of WR 46 is probably not genuine.

As to the long-term variability, we can ascribe the brightening to the WR star itself, since the amplitude of the short-period photometric and line-flux variability increased despite the additional light. This is in accordance with the absence of any spectral feature from a companion. The increase in mean continuum- and mean line flux indicates an increase of the radius of the emission forming layers, which suggests a higher wind density. Since the P-Cygni absorption trough of O v 1371 became deeper without changing the edge-velocity (Fig. 18), and the emission lines do not change their width, we assume that the velocity law remained constant and conclude that the mass-loss rate increased. Thus, the long-term variation of the photometry and the line fluxes indicate a varying *global* density of the wind, as already noted by MAB.

This correlation between brightness and mass-loss rate is in agreement with the relation found by Smith & Maeder (1998) from their analysis of the whole group of WNE stars (note, however, Howarth & Schmutz 1992). Schaerer & Maeder (1992), using a mass-radius relation, derive a luminosity-radius relation. Application of this relation translates the brightness increase of 12% between early 1989 and early 1991 into a radius increase of 4%. This suggestion is in line with the notion that the simultaneous increase of the amplitude of the variability (and small reddening) is interpreted as a radius increase of the various emission forming layers in the wind. Thus, this indicates that the period *decrease* and brightening was accompanied by a radius *increase*; an intriguing clue.

[3] Incidentally, the O vi 3811/34 line was observed by CSH right at the peak of the long-term light curve in December 1991 (Fig. 17), deviating strongly from their model, while normally its strength is about twice as low, in better agreement with their model (see their Fig. 6).

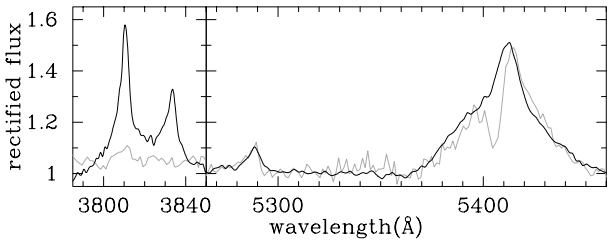

Fig. 19. The emission lines of WR 3 (grey) scaled by a factor of 2.5 to the spectrum of WR 46 (black). Note that the difference with the value of 2.0 as determined by MAB can be attributed to the variability of WR 46. Despite the absence of the O vi 3811/34 line from the spectrum of WR 3, the comparable ratio of O vi 5290 over He ii 5411 for both stars indicates a similar O/He abundance (Sect. 5.2) (spectra by courtesy of Dr. W.-R. Hamann).

6. Summary and discussion

First of all, we note that WR 46 obviously varies on a variety of time scales.The available spectroscopic monitoring data are hardly sufficient to investigate its behaviour in detail. Nevertheless, the variability can be summarized as follows:

1. The line-flux variability mimics the continuum flux variability on the short-term time scale (see also MAB).
2. The line-flux variability has larger relative amplitude than the continuum flux variability.
3. The line-flux variability confirms the large photometric period change between 1989 and 1991.
4. The radial velocity shows (i) obvious variation on a time scale of the photometric double-wave, and (ii) so-called stand-stills (see also MAB).
5. Time-delays are observed from line-to-line in the case of (i) the line-flux variability, (ii) the radial-velocity variation and (iii) the entry of a stand-still, and also (iv) within a single emission line, depending on the height above the continuum. The higher (part of) an emission line is formed in the atmosphere, the larger the time-delay, which is in accordance with the stratified atmosphere of a WR star.
6. He ii 4686 shows, in addition to line-flux and radial-velocity variation, significant line-profile variability on a time scale of the same order as the identified periods.
7. In a total of 17 hours of monitoring, we observed one flare-like event, i.e., in two He ii emission lines a "bump" occurred lasting at most 5 min. And
8. On the long-term time scale of years the line flux follows the photometric behaviour from faint to bright states, which implies that the WR star itself is brightening instead of light from a possible companion.

We conclude that both the short-term and the long-term variabilities identify WR 46 as a Population I WR star, for which the peculiar oxygen abundance is probably not genuine. The short-term variation of the photometry and the line fluxes indicate a varying local density distribution, while the long-term variation is ascribed to a varying global density distribution due to changing mass-loss rate. Thus, despite the coarse resemblance of spectral features and short-term variability, WR 46 has wrongly been suggested to be related to Super Soft X-ray Sources. The following discussion of various aspects of the observed variability may help to understand the cause of the variability.

Time-delays are intrinsic to spectroscopically variable WR stars and studied best in the case of binarity but not limited to binaries alone. An example is provided by the eclipsing WR binary WR 151 (CX Cep, WN4+O5V, $P = 2.13$ d). Lewis et al. (1993) showed that the outer wind lines trail the orbital motion of the inner wind lines. In addition, these authors found a phase-delay up to 0.04 phase (=0.08 d) between the centroid measurements of nearly the whole line relative to the peak of the line. No explanation was put forward. We, here, suggest that the wings of the emission lines are formed more outwards in the wind, and, therefore, trail the central parts of the lines, originating in the inner wind.

Since we cannot determine the period from the radial-velocity measurements, its period may be different from that controlling the photometry, and, probably, the line fluxes. Of course, this would explain the apparent "phase-delays", simply as different phases of different variations, but not the stand-stills. We proposed that the photometric double-wave period controls the light-, the colour-, the line-flux, and the radial-velocity curves, while the last is sometimes disturbed beyond recognition (stand-still) due to the large time-delays. Support was provided by the single observation of the start of a stand still. It was preceded by a radial motion half a period out of phase with respect to the presumed motion of the stellar core. We assume that the phase-delay between the stellar core and the line-emitting regions can grow to be of the order of $\Delta\phi = 0.5$, and that the emission lines then lose the information on the radial velocity of the central object.

We investigate the latter assumption. The time scale of the wind-flow needs to be of the same order as the orbital period. Using the canonical value of $\beta = 1$ in the so-called β-velocity law, the wind flows more than 10 $R_\star$ in one third of the double-wave period. Clearly, this would not fit the assumption above. However, lower acceleration has been suggested for WR stars (e.g., Schmutz 1997; Moffat 1996). According to CSH, a slower velocity law ($\beta \approx 2$) is indicated by the absorption trough of O V 1371, which is formed in the inner wind. For a $\beta = 2$-law the wind travels less than two stellar radii within one third of the period. However, the He II lines, formed further away from the star, do not support such a modification. In this respect it is interesting to note that Hillier & Miller (1999) propose, albeit for much denser WR winds than WR 46 has, a bimodal beta law (inner wind $\beta = 1$ and outer wind $\beta = 50$). Anyway, we suppose that the loss of coherency leading to a stand-still within one or a few orbital revolutions is quite well possible.

Another type of variability of WR 46 is the flare-like behaviour displayed in Fig. 16. Photometric variability on such a time scale for WR stars has been reported by Matthews et al. (1992) in the case of WR 6. These authors found a possible brightning of 1% lasting about ten minutes. Furthermore, Zhilyaev et al. (1991) monitored WR 134 with a time-resolution of 1 s simultaneously in two narrow-band filters tuned to the continuum and to He II 4859, respectively. They observed "saw tooth" flares with a quasi-period of 250 s in the emission line with an amplitude of $0\overset{\mathrm{m}}{.}3$, along with short-lived flares of 5–7 s. As such intense monitoring with high-time resolution has been performed only occasionally and only for known variable WR stars, we cannot address here the significance of the flare-like event in WR 46.

The interpretation of the short- and long-term photometric and spectroscopic variability in terms of pulsation and binarity is deferred to Paper III, where the variability of WR 46 is also compared to that of other WR stars.

Acknowledgements. We are grateful to the colleagues who provided us with spectra of WR 46: Werner Schmutz, Virpi Niemela, Sergey Marchenko. The WN atlas (Hamann et al. 1995b) can presently be found at: `ftp.astro.physik.uni-potsdam.de` in the directory `/pub/hamann/WNatlas`. This research has made use of the Simbad database, operated at CDS, Strasbourg, France.

References

Crowther, P. A., Smith, L. J., & Hillier, D. J. 1995, A&A, 302, 457 (CSH)
Edelson, R. A., & Krolik, J. H. 1988, ApJ, 333, 646
Gies, D. R., Shafter, A. W., & Wiggs, M. S. 1998, AJ, 115, 2566
Hamann, W.-R., Koesterke, L., & Wessolowski, U. 1995a, A&A, 299, 151
Hamann, W.-R., Koesterke, L., & Wessolowski, U. 1995b, A&AS, 113, 459
Hamann, W.-R., & Koesterke, L. 1998, A&A, 333, 251 (HK)
Henize, K. G. 1976, ApJS, 30, 491
Hillier, J. D., & Miller, D. L. 1999, ApJ, 519, 354
Horne, K. 1986, PASP, 98, 609
Howarth, I. D., & Schmutz, W. 1992, A&A, 261, 503
Kahabka, P., & van den Heuvel, E. P. J. 1997, ARA&A, 35, 69
Kato, M., & Hachisu, I. 1994, ApJ, 437, 802
Lewis, D., Moffat, A. F. J., Matthews, J. M., et al. 1993, ApJ, 405, 312
Lockley, J. J., Eyres, S. P., & Wood, J. H. 1997, MNRAS, 287, L14
Marchenko, S. V., Arias, J., Barbá, R., et al. 2000, AJ, 120, 2101 (MAB)
Massey, P., & Conti, P. S. 1981, ApJ, 244, 173
Massey, P., & Conti, P. S. 1983, ApJ, 264, 126
Matthews, J. M., Moffat, A. F. J., & Marchenko, S. V. 1992, A&A, 266, 409
Moffat, A. F. J. 1996, in Wolf-Rayet Stars in the Framework of Stellar Evolution, 33rd Liège Intern. Astroph. Col., ed. J.-M. Vreux, et al., 199

Niemela, V. S., Barbá, R. H., & Shara, M. M. 1995, in Wolf-Rayet stars: Binaries, Colliding Winds, Evolution, ed. K. A. van der Hucht, & P. M. Williams (Kluwer, Dordrecht), IAU Symp. 163, 245
Robert, C., Moffat, A. F. J., Drissen, L., et al. 1992, AJ, 397, 277
Schaerer, D., & Maeder, A. 1992, A&A, 263, 129
Schmutz, W. 1997, A&A, 321, 268
Smith, H. J. 1955, Thesis Harvard College Observatory, 130
Smith, L. F., Shara, M. M., & Moffat, A. F. J. 1996, MNRAS, 281, 163
Smith, L. F., & Maeder, A. 1998, A&A, 334, 845
Steiner, J. E., & Diaz, M. P. 1998, PASP, 110, 276
Veen, P. M., & Wieringa, M. H. 2000, A&A, 363, 1026
Veen, P. M., van Genderen, A. M., van der Hucht, K. A., et al. 2002a, A&A, 385, 585 (Paper I)
Veen, P. M., van Genderen, A. M., & van der Hucht, K. A. 2002b, A&A, 385, 619 (Paper III)
Vreux, J.-M., Dennefeld, M., & Andrillat, Y. 1983, A&AS, 54, 437
Zhilyaev, B. E., Romanyuk, Yu. O., & Svyatogorov, O. A. 1991, Kinemat. Phys. Celest. Bodies, 7, 39